

Archazolid-7-*O*- β -D-glucopyranoside – Isolation, Structural Elucidation and Solution Conformation of a Novel V-ATPase Inhibitor from the Myxobacterium *Cystobacter violaceus*

Dirk Menche,^{*,[a]} Jorma Hassfeld,^[a] Heinrich Steinmetz,^[a] Markus Huss,^[b]
Helmut Wiczorek,^[b] and Florenz Sasse^[c]

Keywords: Natural products / Polyketides / Inhibitors / Glycosides / Archazolid

The novel polyketide macrolide archazolid-7-*O*- β -D-glucopyranoside (**3**) has been isolated from the myxobacterium *Cystobacter violaceus* and the structure of this first archazolid-glycoside has been determined by spectroscopic and degradative methods. A synthesis of simplified 7-*O* analogues, based on regioselective derivatisation of archazolid A, was elaborated. These structurally novel archazolids of natural

and synthetic origin were evaluated in detail for V-ATPase inhibition and their biological activities are discussed in terms of their solution conformations, as determined by high-field NMR studies, including *J*-based conformation analysis and constrained molecular dynamics simulations.
(© Wiley-VCH Verlag GmbH & Co. KGaA, 69451 Weinheim, Germany, 2007)

Introduction

Vacuolar-type ATPases (V-ATPases)^[1] represent an important target from the perspective of medicinal chemistry and drug research, as the function of these proton-translocating proteins is correlated with various diseases such as osteoporosis^[2] and cancer.^[3] The natural products archazolid A (**1**, Figure 1) and archazolid B (**2**), originally isolated by the groups of Höfle and Reichenbach from fermentation broths of the myxobacterium *Archangium gephyra*,^[4–6] represent a novel type of particularly effective inhibitors (IC₅₀ values in the low nanomolar range) of these heteromultimeric enzymes, both in vitro^[7,8] and in vivo.^[6] A high specificity for V-ATPase and a certain selectivity for the mammalian type of this enzyme, together with the reversible mode of binding, add to the attractiveness of these natural polyketides for further development. No analogues for structure–activity studies have so far been described, however, making access to structurally novel archazolid derivatives an important research goal. Of particular interest along these lines are archazolid conjugates, in order either to increase the selectivity for specific types of V-ATPases further

or to allow applications of these antimitotic agents in pro-drug approaches.^[9] Very recently, the stereochemistry of **1** and **2** has been determined by extensive NMR studies and chemical derivatisation.^[10] Here we report on the isolation

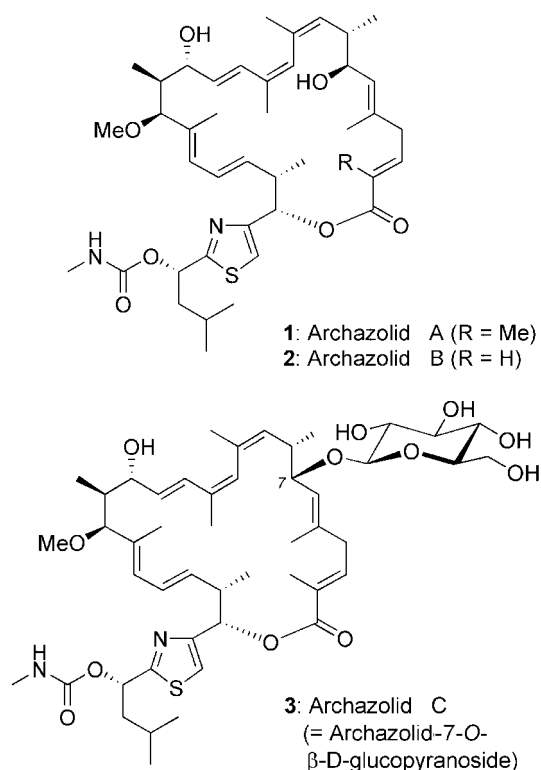


Figure 1. The archazolids: potent V-ATPase inhibitors from myxobacteria.

[a] Helmholtz-Zentrum für Infektionsforschung GmbH, Medizinische Chemie, Inhoffenstrasse 7, 38124 Braunschweig, Germany
Fax: +49-531-6181-9499
E-mail: dirk.menche@helmholtz-hzi.de

[b] Universität Osnabrück, Fachbereich Biologie/Chemie, Abteilung Tierphysiologie, 49069 Osnabrück, Germany

[c] Helmholtz-Zentrum für Infektionsforschung GmbH, Chemische Biologie, Inhoffenstrasse 7, 38124 Braunschweig, Germany

Supporting information for this article is available on the WWW under <http://www.eurjoc.org> or from the author.

and structural elucidation of the first archazolid-glycoside – archazolid-7-*O*- β -D-glucopyranoside (= archazolid C, **3**) – from the myxobacterium *Cystobacter violaceus*.^[11] Furthermore, we also describe the synthesis of simplified 7-*O* analogues and evaluate the inhibitory effects of these structures on V-ATPase in detail. The solution conformation of these novel macrolides is analysed by NMR methods and molecular modelling, allowing the observed biological data to be interpreted.

Results and Discussion

Cystobacter violaceus strain Cb vi105 was identified in a screening for novel and more efficient archazolid-producing myxobacteria. As the archazolids are biologically highly effective compounds that induce a typical rounding of L-929 mouse fibroblast cells, we were able to screen myxobacteria for archazolid production by looking for this special phenotype using low culture volumes (e.g. agar cylinders cut from grown Petri dishes). HPLC analysis of extracts from larger cultures confirmed the presence of archazolid A, together with one major and several further minor metabolites. A 300 L bioreactor cultivation was then run in the presence of Amberlite XAD (1%) for absorption of excreted secondary metabolites. After ten days, the adsorber resin and cell mass (4.9 kg) were harvested by centrifugation and extracted with acetone to give a crude extract (13.7 g), from which consecutive gel chromatography (Sephadex LH-20), MPLC and reversed-phase HPLC yielded archazolid A (**1**, 106 mg) and archazolid C (**3**, 35 mg) as colourless, amorphous solids. All physical and spectroscopic data for **1** were found to be identical to those previously reported for archazolid A from *Archangium gephyra*.^[4,5,10]

The UV/Vis spectrum of the novel metabolite **3** indicated this compound to be an archazolid derivative. The ¹H NMR spectrum of **3** likewise resembled that of **1** (Figure 2, a). In the aromatic region, two one-proton singlets (δ = 5.73 ppm for 11-H, 7.10 ppm for 4'-H), four one-proton doublets (δ = 5.04 ppm: 6-H, 5.36 ppm: 9-H, 6.62 ppm: 13-H, 5.93 ppm: 19-H), and three one-proton doublets (δ = 6.77 ppm: 3-H, 5.71 ppm: 14-H, 6.99 ppm: 20-H, 5.64 ppm: 21-H) suggested a polyunsaturated backbone closely related to that of archazolid A. Likewise, further low-field one-proton signals at δ = 4.42 ppm (7-H), 4.40 ppm (15-H), 3.48 ppm (17-H), 5.96 ppm (23-H) and 5.99 ppm (1'-H) were very similar to those of the parent compound **1**. In the same fashion, all observed three-proton signals for methyl groups resembled the ¹H NMR spectroscopic data for **1**. Further signals in the aliphatic region (chemical shift \leq 3 ppm) at δ = 2.88, 3.04, 2.44, 1.72, and 3.04 ppm were assigned to the macrocyclic protons 4a-H, 4b-H, 8-H, 16-H and 22-H, others at δ = 1.81, 1.88, and 1.77 ppm to the protons in the side chain at C-5' and C-6'. The remaining ¹H NMR signals were observed in the region from δ = 3.00 to 4.00 ppm. This observation, together with HRMS analysis of the novel metabolite, indicating the molecular formula to be C₄₈H₇₂N₂O₁₂S, 162 mass units (correspond-

ing to C₆H₁₀O₅) higher than archazolid A, suggested the presence of a hexose-substituted archazolid. The *O*-glycosidic nature of this compound was also evident from a doublet at δ = 4.17 ppm (7.5 Hz), attributed to an anomeric proton (1'''-H). The signals for 2'''-H to 5'''-H were resolved in CD₃OD and assigned to glucose. The ¹³C NMR spectroscopic data also displayed the expected number of carbons and chemical shifts for glucose,^[12] and this was further confirmed by ROESY interactions.

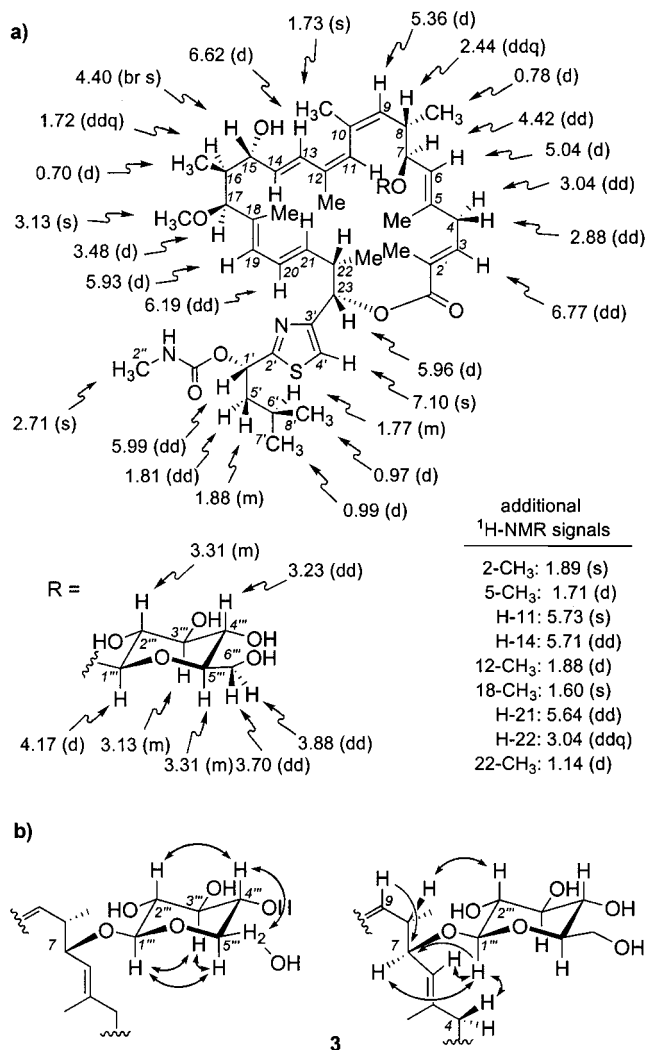
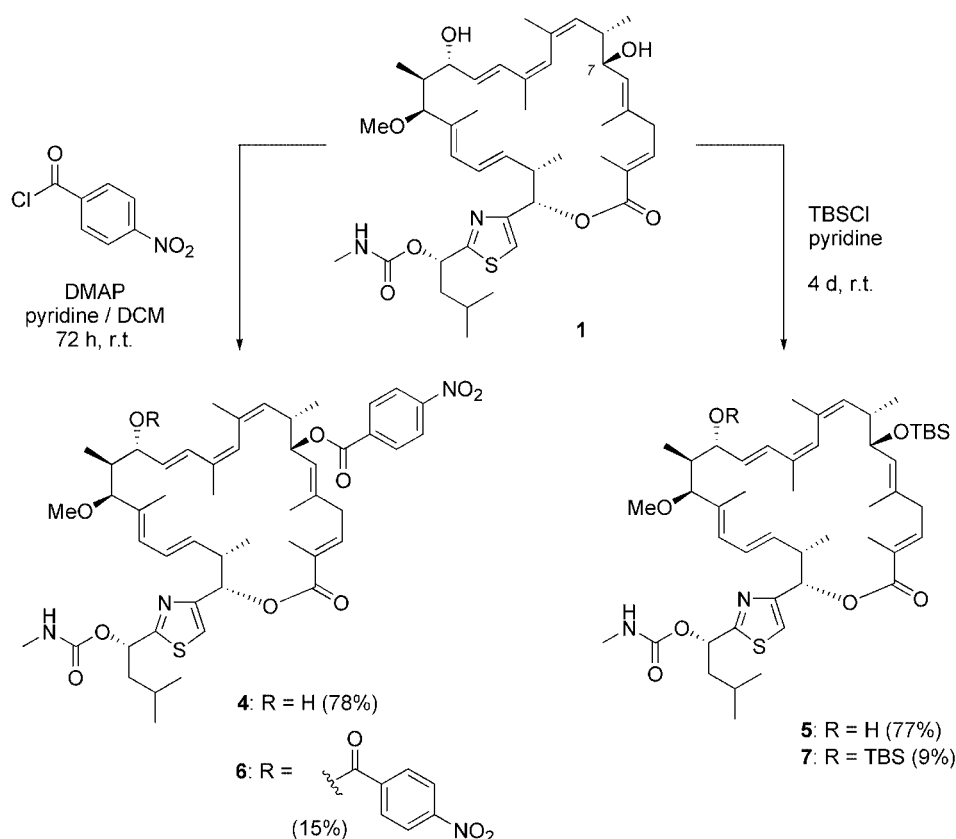


Figure 2. ¹H NMR shifts (δ values in ppm) with multiplet type (a) as well as HMBC (single arrows) and ROESY interactions (double arrows) (b) for the glycoside **3**.

The position of the glucose unit was deduced by ROESY experiments, which showed interactions of 1'''-H and 2'''-H with 6-H, 7-H and 8-H and by a long-range C–H correlation from 1'''-H to C-7. The sugar unit is therefore situated at position C-7, and the new glycoside has the constitution shown in Figure 2. Its structure was further confirmed by TOCSY experiments and by HMBC and HMQC interactions. Further verification of its constitution was obtained by hydrolysis and GC/HPLC comparison with authentic samples of glucose and archazolid. For the new glycoside, we suggest the name archazolid C.



Scheme 1. Synthesis of the 7-*O* analogues **4** and **5** by selective functionalization of archazolid A (**1**).

Access to sufficient material of archazolid A from the myxobacterium *Cystobacter violaceus* opened the possibility of rationally elaborating a synthesis of simplified 7-*O* analogues of archazolid C and thus of obtaining further structure–activity data for this novel metabolite. This approach would require a selective derivatisation of the 7-*O*-group in the presence of the free hydroxy moiety at C-15. This indeed seemed feasible with respect to the recently determined solution conformation of **1**,^[10] which indicates the 7-OH to be readily accessible. To test our ideas for such a regioselective functionalisation, archazolid A was treated with electrophiles possessing a space demand similar to that of glucose to provide derivatives **4** and **5** in order to allow for meaningful SAR data (Scheme 1). After optimisation of the reaction conditions, both a selective esterification and a selective silylation could be effected, and the *para*-nitrobenzoate **4** and the silyl ether **5** were obtained as the major products together with only minor amounts of the bis-adducts **6** and **7**. No monofunctionalization at 15-OH was observed, showing the 7-hydroxy to be more reactive.

This efficient synthesis of the 7-*O* analogues enabled access to sufficient material for assessment of their biological activities in parallel with the evaluation of archazolid C. In view of the recently discovered high anti-V-ATPase activity of archazolids A and B,^[5,7] the inhibitory efficacies of the novel analogues **3–5** on purified V-ATPase holoenzyme from the mid-gut of the tobacco hornworm were tested (Table 1). All the new analogues showed very similar de-

grees of inhibition in this in vitro test system, but these activities are dramatically reduced in relation to those of **1** and **2**, which suggests that a free 7-OH is an important part of the pharmacophore.

Table 1. Inhibition of the V_1/V_o holoenzyme activity and cytotoxicities of archazolids A–C and their analogues **4** and **5**.

	Enzyme inhibition V_1/V_o holoenzyme: IC_{50} , nmol/mg enzyme ^[a]	Growth inhibition L-929: IC_{50} , nM ^[d]
Archazolid A (1)	0.6 ^[b]	0.81
Archazolid B (2)	0.6 ^[c]	1.1
Archazolid C (3)	210	1600
Analogue 4	250	290
Analogue 5	140	940

[a] The specific enzyme activity of the controls without inhibitors was $1.5 \pm 0.2 \mu\text{mol mg}^{-1} \text{min}^{-1}$. [b] 0.8 nmol/mg enzyme corresponds to 10 nM. [c] Value taken from ref.^[7]. [d] Origin of the mammalian cell line: murine connective tissue DSM ACC 2.

These in vitro data are consistent with the corresponding inhibitory effects on the growth of the murine connective tissue cell line L-929. While the IC_{50} values for **1** and **2** are in the low nanomolar range, the analogues are less potent, with IC_{50} values two to three magnitudes higher. Among the analogues tested, the benzoate **4** was three times more potent than the silyl analogue **5**, and five times more active than the glycoside **3**. The growth inhibitory activity does not run in parallel with the activity at the target enzyme; this may be the result of different membrane permeabilities.

To allow further analysis of these biological data, the solution conformations of archazolid-7-*O*- β -D-glucopyranoside and its 7-*O* analogues were studied by NMR spectroscopy. As close mimics of biologically relevant systems, and also for consistency with a previous analysis of archazolid A,^[10] these compounds were studied in CD₃OD, in which optimum ¹H NMR signal dispersion was achieved at the highest available field strength (600 MHz). A combination of multiplet analysis,^[13] homonuclear decoupling and TOCSY experiments at different mixing times (Figure 2) were used for determination of all ³J_{H,H} coupling constants, and information on the spatial relationships between non-adjacent protons was deduced from ROESY experiments. Within the macrocyclic core, all analogues show a characteristic sequence of large (>8 Hz) and small (<4 Hz) ³J_{H,H} coupling constants, together with a series of highly specific transannular NOE correlations, which indicate a high degree of structural rigidity for the macrocycle. Within this lactone ring, a certain degree of flexibility only has to be considered around the (22,23)-bond, as suggested by a medium coupling from 22-H to 23-H, and to a lesser degree also around the (2,23)-bond, which is indicated by a broadening of the corresponding ¹H NMR signals. This behaviour is in close agreement with the previously determined flexibility of archazolid A. Selected key coupling constants for the “western” (row 1–5, 3-H...9-H), the “northeastern” (row 6–8, 14-H...17-H) and the “southeastern” fragments (row 9–11, 19-H...23-H) of the macrocycle, as well as for attachment of the side chain (row 12–13, 1'-H...5'b-H) in comparison to the data for archazolids A and B are depicted in Table 2. These values show a very high degree of similarity for all the archazolids, which indicate that all these structures reside in a highly conserved solution conformation. Notably, variation of the 7-*O*-substituent appears to have no significant influence on the observed conformation.

Table 2. Selected ^{1,3}J_{H,H} coupling constants for archazolids A (1) and C (3) and analogues 4 and 5.

	1	3	4	5
3-H to 4a-H	7.5	7.4	7.2	6.8
3-H to 4b-H	7.5	7.4	8.1	8.3
6-H to 7-H	9.5	9.8	10.0	9.1
7-H to 8-H	9.4	9.8	9.7	8.9
8-H to 9-H	9.6	9.1	9.6	10.1
14-H to 15-H	6.0	5.3	7.5	7.2
H-15 to H-16	3.2	3.2	3.2	4.2
16-H to 17-H	9.0	8.9	8.5	8.7
19-H to 20-H	10.9	10.6	10.8	10.6
21-H to 22-H	7.0	6.2	7.4	7.6
22-H to 23-H	4.1	3.8	5.3	4.5
1'-H to 5'a-H	9.1	9.1	8.7	9.1
1'-H to 5'b-H	4.5	4.5	4.5	4.5

Input files with constrained torsion angles and distances based on these spectroscopic data were generated for archazolid C in MacroModel 8.5^[14] and subjected to restrained Monte Carlo 10,000-step conformational searches (MM2 force field) with the generalised Born/surface area (CB/SA)

water solvent model^[15] to reveal the conformation as depicted in Figure 3 as the global solution conformation minimum within a series of discrete families of structurally related low-energy conformations within 5 kcal mol⁻¹, which is closely consistent with data previously determined for archazolid A.^[10] Archazolid C thus likewise resides in an “open” and fairly planar shape. Flexibility was observed around the (22,23)-bond and to a lesser degree also around the (15,16)-bond and within the side chain, whilst the remaining part of the macrocycle is predicted to be rather rigid.

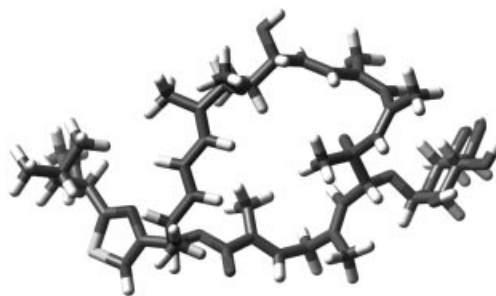


Figure 3. Preferred solution conformation of archazolid C (3).

Conclusions

In summary, we have described the first archazolid-glycoside, archazolid C (3), from the myxobacterium *Cystobacter violaceus*. Its constitution was established by NMR investigations and unambiguously confirmed by acidic cleavage. Simplified 7-*O* analogues were prepared by a highly regioselective *O*-functionalization of archazolid A. Whilst each of these novel archazolids adopts a solution conformation very similar to that of archazolid A, the inhibitory effects on V-ATPase are reduced by an order of three magnitudes, which suggests that a free 7-OH is part of the pharmacophoric region. This highly reduced activity of the 7-*O* analogues, together with their synthetic availability from 1, might enable applications in detoxified prodrug approaches.^[9] Furthermore, these results show that it is possible to modify the structure of archazolid while retaining the overall shape and flexibility and suggest that it could also be possible to increase its potency while retaining its 3D shape.

Experimental Section

General Remarks: Optical rotations were determined with a Perkin–Elmer 241 instrument, UV spectra were recorded with a Shimadzu UV-2102 PC scanning spectrometer, and IR spectra were measured with a Nicolet 20DXB FT-IR spectrometer. NMR spectra were recorded in CD₃OD and CDCl₃ with a Bruker DMX 600 and a Bruker WM 400 spectrometer. EI and DCI mass spectra (reactant gas ammonia) were obtained with a Finnigan MAT 95 spectrometer; high resolution data were acquired by peak matching (M/DM = 10000). Pure compounds were characterized by analytical HPLC on Nucleosil C 18 (column 125 × 2 mm, 5 μm, flow 0.3 mL min⁻¹), diode array detection. Preparative HPLC on Nucleosil (column

250 × 21 mm, 7 µm, flow 18 mL min⁻¹), detection: UV absorption at 254 nm. Analytical TLC [TLC aluminium sheets silica gel Si 60 F₂₅₄ (Merck)], solvent: mixtures of ethyl acetate/petroleum ether, detection: UV absorption at 254 nm, dark blue spots on staining with cerium(IV) sulfate/phosphomolybdic acid in sulfuric acid followed by charring.

Isolation of Archazolid A (1) and C (3) from *Cystobacter violaceus*:

A fermentation batch (300 L) of strain Cb vi105, isolated at GBF (Braunschweig, Germany), was grown in M7 medium in the presence of Amberlite XAD-16 adsorber resin (3 L) at 30 °C.^[5] After harvesting by centrifugation, the mixture of wet cell mass and adsorber resin was extracted with four batches of acetone (each 3 L) by stirring, sedimentation and decanting. The extract was concentrated on a rotary evaporator (30 °C/50 mbar) to the water phase, which was extracted with ethyl acetate (one portion of 3.5 L and two portions of 1.5 L). The organic phase was evaporated (30 °C/150 mbar) to the water phase. The residue was dissolved in methanol (1 L) and washed three times with heptane (1 L). Evaporation gave the crude extract (13.7 g), which was dissolved in methanol for further purification by gel chromatography on Sephadex LH 20 (Fluka, Steinheim, solvent: methanol, flow 7 mL min⁻¹). Further purification by medium pressure RP chromatography (solvent: methanol/water 8:2, detection 230 nm, flow 65 mL min⁻¹) and high pressure RP chromatography (solvent: acetonitrile/water 65/35, detection 230 nm, flow 15 mL min⁻¹) gave archazolid A (106 mg) and archazolid C (35 mg). These antibiotics were analysed by HPLC (methanol/water 82:18, flow rate: 0.3 mL min⁻¹, detection: diode array). The retention times were 11.8 min for archazolid A and 6.3 min for archazolid C.

Archazolid A (1): Colourless, amorphous solid: t_R = 11.8 min (Nucleosil C18, 125 × 2 mm, 5 µm, methanol/water 82:18, flow rate: 0.3 mL min⁻¹, diode array detection); R_f = 0.25 (silica gel Si 60 aluminium sheets, petroleum ether/ethyl acetate 2:1). $[α]_D^{25}$ = -64.0 (c = 12.8 mg mL⁻¹, MeOH). IR (KBr): $\tilde{\nu}_{max}$ = 3500, 2944, 2876, 1720, 1254, 1143 cm⁻¹. UV (MeOH): λ_{max} (lg ϵ) 228 nm (4.6). The NMR spectroscopic data were identical to those previously published.^[4,5,10]

Archazolid C (3): Colourless, amorphous solid: t_R = 6.6 min (Nucleosil C18, 125 × 2 mm, 5 µm, acetonitrile/water 65:35, flow rate: 0.3 mL min⁻¹, diode array detection). $[α]_D^{25}$ = -33.9 (c = 6.2 mg mL⁻¹, MeOH). ¹H NMR (CD₃OD, 600 MHz): δ = 0.70 (d, J = 7.2 Hz, 3 H, 16-CH₃), 0.78 (d, J = 6.8 Hz, 3 H, 8-CH₃), 0.97 (d, J = 6.8 Hz, 3 H, 7'-H₃), 0.99 (d, J = 6.8 Hz, 3 H, 8'-H₃), 1.14 (d, J = 6.8 Hz, 3 H, 22-CH₃), 1.60 (s, 3 H, 18-CH₃), 1.71 (s, 3 H, 5-CH₃), 1.72 (ddq, J = 8.9, 3.2, 7.2 Hz, 1 H, 16-H), 1.73 (s, 3 H, 10-CH₃), 1.77 (m, 1 H, 6'-H), 1.81 (dd, J = 7.9, 4.9 Hz, 1 H, 5'-H), 1.88 (m, 1 H, 5'-H), 1.88 (d, J = 1.1 Hz, 3 H, 12-CH₃), 1.89 (s, 3 H, 2-CH₃), 2.44 (ddq, J = 9.8, 9.1, 6.8 Hz, 1 H, 8-H), 2.71 (s, 3 H, 2'-H₃), 2.88 (dd, J = 14.3, 6.8 Hz, 1 H, 4-H), 3.04 (ddq, J = 6.2, 3.8, 6.8 Hz, 1 H, 22-H), 3.04 (dd, J = 14.3, 7.9 Hz, 1 H, 4-H), 3.13 (s, 3 H, 17-OCH₃), 3.23 (dd, J = 8.5, 8.5 Hz, 1 H, 4'''-H), 3.31 (m, 1 H, 5'''-H), 3.31 (m, 1 H, 2'''-H), 3.48 (brd, J = 8.9 Hz, 1 H, 17-H), 3.70 (dd, J = 11.7, 5.9 Hz, 1 H, 6'''-H), 3.88 (dd, J = 11.7, 2.3 Hz, 1 H, 6'''-H), 4.17 (d, J = 7.5 Hz, 1 H, 1'''-H), 4.40 (brs, 1 H, 15-H), 4.42 (dd, J = 9.8, 9.8 Hz, 1 H, 7-H), 5.04 (d, J = 9.8 Hz, 1 H, 6-H), 5.36 (d, J = 9.1 Hz, 1 H, 9-H), 5.64 (dd, J = 15.3, 6.2 Hz, 1 H, 21-H), 5.71 (dd, J = 16.2, 5.3 Hz, 1 H, 14-H), 5.73 (s, 1 H, 11-H), 5.93 (d, J = 10.6 Hz, 1 H, 19-H), 5.96 (d, J = 3.8 Hz, 1 H, 23-H), 5.99 (dd, J = 9.1, 4.5 Hz, 1 H, 1'-H), 6.19 (dd, J = 14.9, 11.1 Hz, 1 H, 20-H), 6.62 (d, J = 15.9 Hz, 1 H, 13-H), 6.77 (t, J = 7.4 Hz, 1 H, 3-H), 7.10 (dd, s, 1 H, 4'-H) ppm. ¹³C NMR (CD₃OD, 101 MHz): δ = 12.5 (Me-18), 12.6 (Me-16), 12.8

(Me-2), 17.2 (Me-5), 17.3 (Me-22), 17.9 (Me-8), 20.2 (Me-12), 22.5 (C-7'), 23.5 (C-8'), 24.8 (Me-10), 26.0 (C-6'), 27.7 (C-2''), 39.5 (C-8), 40.4 (C-4), 40.7 (C-22), 43.7 (C-16), 46.1 (C-5'), 56.4 (17-OMe), 63.2 (C-6'''), 72.0 (C-5'''), 73.5 (C-1'), 74.3 (C-15), 75.1 (C-4'''), 77.3 (C-7), 77.5 (C-23), 78.3 (C-3'''), 78.7 (C-2'''), 89.8 (C-17), 100.3 (C-1'''), 116.5 (C-4'), 127.3 (C-6), 127.7 (C-20), 129.4 (C-13), 130.0 (C-2), 130.7 (C-11), 130.7 (C-19), 133.3 (C-10), 133.4 (C-9), 133.4 (C-12), 134.0 (C-14), 134.9 (C-21), 135.6 (C-18), 141.0 (C-5), 142.1 (C-3), 156.3 (C-3'), 158.5 (C-1''), 168.4 (C-1), 174.2 (C-2') ppm. The ¹³C assignments were achieved by HMQC and HMBC experiments. IR (film): $\tilde{\nu}_{max}$ = 3389, 2931, 1717, 1079 cm⁻¹. UV(MeOH): λ_{max} (lg ϵ) 229 nm (5.2). HRMS for C₄₈H₇₂N₂O₁₂NaS [M + Na]⁺: calcd. 923.4704; found: 923.4704.

Hydrolysis of Archazolid C: a) Glucose was detected as the completely TMS-silylated methyl glycoside by Chaplin's method.^[16] b) Preparative scale. Compound 3 (1.00 mg, 1.1 µmol) was stirred in HCl/MeOH (0.5 M, 3 mL) at 50 °C for 30 min. Sat. aq. NaHCO₃ (3 mL) and EtOAc (4 mL) were added, the organic phase was separated, and the aqueous phase was extracted with EtOAc. Drying of the combined organic phases (MgSO₄), concentration of the organic phase and purification by high pressure RP chromatography (solvent: acetonitrile/water 65:35, detection 230 nm, flow 15 mL min⁻¹) gave archazolid A (0.5 mg, 0.7 µmol). The chromatographic (HPLC) and spectroscopic (¹H NMR) data were identical to those for the authentic natural product.

7-O-*p*-Nitrobenzoate of Archazolid A (4): A solution of archazolid A (9.7 mg, 13.1 µmol) in DCM (0.5 mL) was treated at room temperature with pyridine (0.25 mL), catalytic amounts of DMAP and *p*-nitrobenzoyl chloride (24.4 mg, 131 µmol) and the mixture was stirred at this temperature for 24 h. The reaction mixture was filtered through SiO₂ (elution with DCM) and washed twice with sat. aq. NaHCO₃ (10 mL) and once with water (5 mL). Drying of the organic phase (Na₂SO₄), evaporation of the solvent and flash chromatography on SiO₂ (petroleum ether/ethyl acetate 4:1 to 7:1) gave the dibenzoate 6 (1.9 mg, 2.0 µmol, 15%, Supporting Information) and the monobenzoate 4 (9.1 mg, 10.2 µmol, 78%). **4:** R_f = 0.32 (silica gel Si 60 aluminium sheets, petroleum ether/ethyl acetate 2:1). $[α]_D^{25}$ = +13.3 (c = 10.3 mg mL⁻¹, CHCl₃). ¹H NMR (CD₃OD, 600 MHz): δ = 0.79 (d, J = 7.0 Hz, 3 H, 16-CH₃), 1.04 (m, J = 6.8 Hz, 3 H, 8-CH₃), 0.98 (d, J = 6.8 Hz, 7'-H₃), 1.00 (d, J = 6.8 Hz, 8'-H₃), 1.11 (d, J = 6.8 Hz, 3 H, 22-CH₃), 1.64 (s, 3 H, 18-CH₃), 1.65 (s, 3 H, 10-CH₃), 1.72 (ddq, J = 8.5, 3.2, 7.0 Hz, 16-H), 1.77 (m, 6'-H), 1.82 (m, 5'-H), 1.86 (m, 5'-H), 1.89 (d, J = 0.8 Hz, 3 H, 5-CH₃), 1.91 (s, 3 H, 2-CH₃), 1.99 (d, J = 0.9 Hz, 3 H, 12-CH₃), 2.69 (ddq, J = 9.7, 9.6, 6.8 Hz, 8-H), 2.75 (s, 2'-H₃), 2.88 (dd, J = 14.3, 7.2 Hz, 4-H), 3.04 (ddq, J = 7.4, 5.3, 6.8 Hz, 22-H), 3.06 (dd, J = 14.3, 7.9 Hz, 4-H), 3.17 (s, 3-H, 17-OCH₃), 3.31 (d, J = 8.5 Hz, 1 H, 17-H), 4.30 (dd, J = 8.2, 3.2 Hz, 1 H, 15-H), 5.22 (d, J = 9.6 Hz, 1 H, 9-H), 5.29 (d, J = 10.0 Hz, 1 H, 6-H), 5.51 (dd, J = 15.4, 7.3 Hz, 1 H, 21-H), 5.53 (dd, J = 9.7, 9.7 Hz, 1 H, 7-H), 5.69 (s, 1 H, 11-H), 5.80 (d, J = 11.1 Hz, 1 H, 19-H), 5.88 (dd, J = 16.0, 7.5 Hz, 1 H, 14-H), 5.96 (d, J = 5.3 Hz, 1 H, 23-H), 6.03 (dd, J = 8.7, 4.5 Hz, 1 H, 1'-H), 6.13 (dd, J = 15.4, 10.8 Hz, 1 H, 20-H), 6.45 (d, J = 15.6 Hz, 1 H, 13-H), 6.81 (dd, J = 8.1, 7.2 Hz, 1 H, 3-H), 7.20 (s, 1 H, 4'-H), 8.26 (d, J = 9.0 Hz, 2 H, PNB-H₂), 8.40 (d, J = 9.0 Hz, 2 H, PNB-H₂) ppm. ¹³C NMR (CDCl₃, 101 MHz): δ = 11.6 (Me-18), 12.4 (Me-2), 13.7 (Me-16), 16.4 (Me-8), 17.1 (Me-5), 17.5 (Me-22), 19.9 (Me-12), 24.3 (Me-10), 24.4 (C-6'), 24.2 (C-7'), 24.6 (C-8'), 27.6 (C-2''), 38.7 (C-8), 39.4 (C-4), 40.7 (C-22), 41.8 (C-16), 44.3 (C-5'), 56.2 (30-OMe), 72.2 (C-1'), 76.2 (C-23), 75.8 (C-15), 76.5 (C-7), 90.6 (C-17), 115.5 (C-4'), 123.5 (PNB-C), 124.1 (C-6), 126.3 (C-20), 128.5 (C-13), 128.9 (C-19), 129.1 (C-11), 129.8 (C-9), 130.0 (C-2), 130.6 (PNB-

C), 132.4 (C-14), 133.3 (C-10), 133.3 (C-12), 134.9 (C-21), 135.5 (C-18), 135.9 (PNB-C), 139.7 (C-3), 139.8 (C-5), 149.6 (PNB-C), 155.9 (C-3'), 158.4 (C-1''), 164.1 (PNB-C=O), 167.3 (C-1), 171.2 (C-2') ppm. The ^{13}C assignments were achieved by HMQC and HMBC experiments. HRMS for $\text{C}_{49}\text{H}_{65}\text{N}_3\text{O}_{10}\text{SNa}$ [$\text{M} + \text{Na}$] $^{+}$: calcd. 910.4288; found: 910.4280.

7-*O*-TBS-Archazolid A (5): A solution of archazolid A (**1**, 30.0 mg, 40.7 μmol) in DCM (1 mL) and pyridine (0.5 mL) was treated at room temperature with TBSCl (36.7 mg, 245 μmol) and the mixture was stirred at this temperature for 72 h. The reaction mixture was filtered through SiO_2 (elution with DCM). Evaporation of the solvent and flash chromatography (petroleum ether/ethyl acetate 10:1 to 5:1 to 2:1) gave 3.4 mg (3.5 μmol , 8.6%) of the (7,15)-bis-*O*-TBS-ether of archazolid A (**7**, see Supporting Information) and the mono-TBS ether **5** (26.7 mg, 31.3 μmol , 77%). 7-*O*-TBS-archazolid A (**5**): Colourless oil; R_f = 0.35 (silica gel Si 60 aluminium sheets, petroleum ether/ethyl acetate 2:1). $[\alpha]_D^{25}$ = -74.9 (c = 7.3 mg mL^{-1} , CHCl_3). ^1H NMR (CD_3OD , 600 MHz): δ = 0.03 (s, 3 H, Si- CH_3), 0.06 (s, 3 H, Si- CH_3), 0.78 (d, J = 7.3 Hz, 3 H, 16- CH_3), 0.88 (d, J = 6.8 Hz, 3 H, 8- CH_3), 0.91 [s, 9 H, Si- $\text{C}(\text{CH}_3)_3$], 1.01 (d, J = 6.80 Hz, 3 H, 8'- H_3), 1.03 (d, J = 6.4 Hz, 3 H, 7'- H_3), 1.12 (d, J = 6.8 Hz, 3 H, 22- CH_3), 1.61 (d, J = 1.1 Hz, 3 H, 18- CH_3), 1.72 (d, J = 1.1 Hz, 3 H, 5- CH_3), 1.75 (ddq, J = 8.7, 4.2, 6.8 Hz, 1 H, 16-H), 1.78 (s, 3 H, 10- CH_3), 1.80 (m, 2 H, 5'-H, 6'-H), 1.84 (dd, J = 8.3, 4.9 Hz, 1 H, 5'-H), 1.91 (s, 3 H, 2- CH_3), 1.93 (d, J = 1.1 Hz, 3 H, 12- CH_3), 2.30 (ddq, J = 9.8, 8.6, 6.8 Hz, 1 H, 7-H), 2.74 (s, 3 H, 2'- H_3), 2.95 (dd, J = 15.1, 6.8 Hz, 1 H, 4-H), 3.00 (dd, J = 14.4, 9.1 Hz, 1 H, 4-H), 3.06 (ddq, J = 7.6, 4.5, 6.8 Hz, 1 H, 22-H), 3.13 (s, 3 H, 17- OCH_3), 3.29 (d, J = 8.7 Hz, 1 H, 17-H), 4.08 (dd, J = 8.9, 8.9 Hz, 1 H, 7-H), 4.20 (dd, J = 7.2, 4.2 Hz, 1 H, 15-H), 5.16 (dt, J = 10.1, 1.2 Hz, 1 H, 9-H), 5.19 (d, J = 9.1 Hz, 1 H, 6-H), 5.55 (dd, J = 15.1, 7.6 Hz, 1 H, 21-H), 5.80 (dd, J = 15.9, 7.9 Hz, 1 H, 14-H), 5.80 (s, 1 H, 11-H), 5.83 (d, J = 9.4 Hz, 1 H, 19-H), 5.96 (d, J = 4.5 Hz, 1 H, 23-H), 6.03 (dd, J = 9.1, 4.9 Hz, 1 H, 1'-H), 6.06 (dd, J = 14.7, 10.6 Hz, 1 H, 20-H), 6.38 (d, J = 15.9 Hz, 1 H, 13-H), 6.87 (ddd, J = 8.3, 6.8, 1.5 Hz, 1 H, 3-H), 7.20 (s, 1 H, 4'-H) ppm. ^{13}C NMR (CDCl_3 , 101 MHz): δ = -4.71 (Si- CH_3), -4.20 (Si- CH_3), 11.4 (Me-18), 12.6 (Me-2), 13.8 (Me-16), 14.4 [Si- $\text{C}(\text{CH}_3)_3$], 16.6 (Me-5), 16.9 (Me-8), 17.7 (Me-22), 19.83 (Me-12), 22.2 (C-7'), 23.0 (C-8'), 24.4 (Me-10), 24.7 (C-6'), 25.9 [SiC(CH $_3$) $_3$], 27.6 (C-2''), 39.8 (C-4), 40.8 (C-22), 41.1 (C-8), 42.0 (C-16), 44.4 (C-5'), 56.1 (30- OCH_3), 72.1 (C-1'), 73.8 (C-7), 76.2 (C-15), 76.3 (C-23), 90.5 (C-17), 115.1 (C-4'), 126.3 (C-20), 128.6 (C-2), 128.8 (C-13), 129.3 (C-19), 130.5 (C-11), 130.6 (C-6), 131.6 (C-14), 132.3 (C-9), 132.3 (C-10), 133.0 (C-12), 133.2 (C-18), 134.6 (C-21), 140.8 (C-3), 141.1 (C-5), 155.2 (C-3'), 156.0 (C-1''), 168.3 (C-1), 174.3 (C-2') ppm. The ^{13}C assignments were achieved by HMQC and HMBC experiments. HRMS for $\text{C}_{48}\text{H}_{76}\text{N}_2\text{O}_7\text{NaSSi}$ [$\text{M} + \text{Na}$] $^{+}$: calcd. 875.5040; found: 875.5050.

Molecular Dynamics Simulations: Files with constrained torsion angles and H-H distances based on the spectral analysis were generated in MacroModel 8.5.^[14] Restrained molecular modelling studies were performed with the MMFFs force field, together with the generalised Born/Surface area (GB/SA) water solvent model.^[15] Structures were subjected to a minimisation procedure to the nearest local minimum prior to the generation of new local energy conformers by Monte Carlo searching (20,000 steps). All conformations within 50 kJ mol^{-1} were recorded. The normal setup protocol was employed, with experiments sampling batches of 1000 to 2000 structures.

Cell Culture and Growth Inhibition Assay: The L-929 mouse cell line was from the German collection of Microorganisms and Cell

Cultures (DSMZ) and cultivated in DME medium (GIBCO BRL) plus newborn calf serum (10%) and CO_2 (10%) at 37 $^{\circ}\text{C}$ in a moist atmosphere. Growth inhibition was measured on microtiterplates. Aliquots of 120 μL of the suspended cells ($50,000 \text{ mL}^{-1}$) were added to 60 μL of a serial dilution of the inhibitor. After 5 d, metabolic activity per well was determined by the MTT assay.^[17]

V-ATPase Assays: V-ATPase was purified by published procedures.^[18] Standard V-ATPase assays with a final volume of 160 μL and a pH of 8.1 consisted of protein (3 μg), Tris-MOPS (50 mM), 2-mercaptoethanol (3 mM), MgCl_2 (1 mM), KCl (20 mM), $\text{C}_{12}\text{E}_{10}$ (0.003%), NaCl (20 mM), and Tris-HCl (3 mM). After 5 min of pre-incubation at 30 $^{\circ}\text{C}$ with or without inhibitors, Tris-ATP (1 mM) was added and after incubation for 2 min, the reaction was stopped by placing the tube in liquid nitrogen. Inorganic phosphate produced in the assays of V-ATPase was measured according to the protocol of Wiczorek et al.^[19]

Supporting Information (see also the footnote on the first page of this article): Complete spectroscopic data for **1**, **6** and **7**, calculated data and copies of NMR spectra for archazolid C.

Acknowledgments

We thank the Fonds der Chemischen Industrie ("Liebig-Stipendium" to D. M.) and the Volkswagenstiftung (Funding Initiative: "Interplay between Molecular Conformations and Biological Function") for generous funding. In addition, this work was supported by the Helmholtz-Zentrum für Infektionsforschung GmbH (HZI) and the Deutsche Forschungsgemeinschaft (DFG) (SFB 431). Particular thanks are due to Antje Ritter, Tatjana Arnold and Bettina Hinkelmann for technical support and the Fermentation Service of the HZI for help with large scale fermentation. Furthermore, we also thank C. Kakoschke and B. Jaschok-Kentner and C. Hanko for recording NMR and mass spectra, Dr. V. Wray for helpful discussions and Dr. M. Nimtz for GC-MS analysis of glucose.

- [1] H. Wiczorek, D. Brown, S. Grinstein, J. Ehrenfeld, W. R. Harvey, *Bioessays* **1999**, *21*, 637–648; T. Nishi, M. Forgac, *Nat. Rev. Mol. Cell Biol.* **2002**, *3*, 94–103.
- [2] P. H. Schlesinger, H. C. Blair, S. L. Teitelbaum, J. C. Edwards, *J. Biol. Chem.* **1997**, *272*, 18636–18643.
- [3] S. R. Sennoune, D. Luo, R. Martinez-Zaguilan, *Cell. Biochem. Biophys.* **2004**, *40*, 185–206.
- [4] G. Höfle, H. Reichenbach, F. Sasse, H. Steinmetz, German Patent DE 4142951C1, **1993**.
- [5] F. Sasse, H. Steinmetz, G. Höfle, H. Reichenbach, *J. Antibiot.* **2003**, *56*, 520–525.
- [6] For a review on cytotoxic secondary metabolites from myxobacteria, see: H. Reichenbach, G. Höfle, in: *Drug Discovery from Nature* (Eds.: S. Grabley, R. Thiercke), Springer Verlag, Berlin, **1999**, pp. 149–179.
- [7] M. Huss, F. Sasse, B. Kunze, R. Jansen, H. Steinmetz, G. Ingenhorst, A. Zeeck, H. Wiczorek, *BMC Biochemistry* **2005**, *6*, 13; <http://www.biomedcentral.com/1471-2091-6-13>.
- [8] Archazolid A has been found to bind to the membrane-bound V_o subunit c: see ref.^[7]. This subunit forms an oligomer, building up a ring structure of six or more copies, which transports protons across the membrane. In addition, Murata et al. recently described the structure of the ring from a bacterial V-ATPase at 2.1 \AA resolution and showed that 10 copies form the c ring. These results make a detailed study on the 3D structure of novel inhibitors, such as the one described here, a rewarding task: T. Murata, I. Yamato, Y. Kakinuma, A. G. Leslie, J. E. Walker, *Science* **2005**, *308*, 654–659; see also: T. Nishi, M. Forgac, *Nat. Rev. Mol. Cell Biol.* **2002**, *3*, 94–103.

- [9] For illustrative references along these lines, see: S. R. Roffler, S. M. Wang, J. W. Chern, M. Y. Yeh, E. Tung, *Biochem. Pharmacol.* **1991**, *42*, 2062–2065; L. F. Tietze, R. Hannemann, W. Buhr, M. Lögers, P. Menningen, M. Lieb, D. Starck, T. Grote, A. Döring, I. Schuberth, *Angew. Chem. Int. Ed. Engl.* **1996**, *35*, 2674–2677.
- [10] J. Hassfeld, C. Farès, H. Steinmetz, T. Carlomagno, D. Menche, *Org. Lett.* **2006**, *8*, 4751–4754.
- [11] No chemical analyses of the secondary metabolites of this myxobacterial species have previously been reported.
- [12] S. Seo, Y. Tomita, K. Tori, Y. Yoshimura, *J. Am. Chem. Soc.* **1978**, *100*, 3331–3339.
- [13] T. R. Hoye, P. R. Hanson, J. R. Vyvyan, *J. Org. Chem.* **1994**, *59*, 4096–4103; T. R. Hoye, H. Zhao, *J. Org. Chem.* **2002**, *67*, 4014–4016.
- [14] F. Mohamadi, N. G. J. Richards, W. C. Guida, R. Liskamp, M. Lipton, C. Caufield, G. Chang, T. Hendrickson, W. C. Still, *J. Comput. Chem.* **1990**, *11*, 440–467.
- [15] W. C. Still, A. Tempczyk, R. C. Hawley, T. Hendrickson, *J. Am. Chem. Soc.* **1990**, *112*, 6127–6129.
- [16] M. F. Chaplin, *Anal. Biochem.* **1982**, *123*, 336–341.
- [17] T. Mosman, *J. Immunol. Methods* **1983**, *65*, 55–63.
- [18] M. Huss, G. Ingenhorst, S. König, M. Gassel, S. Dröse, A. Zeeck, K. Altendorf, H. Wiczorek, *J. Biol. Chem.* **2002**, *277*, 40544–40548.
- [19] H. Wiczorek, M. Cioffi, U. Klein, W. R. Harvey, H. Schweikl, M. G. Wolfersberger, *Methods Enzymol.* **1990**, *192*, 608–616.

Received: October 18, 2006

Published Online: January 12, 2007